IEEE Robotics and Automation Letters (RAL) paper presented at the
2020 IEEE/RSJ International Conference on Intelligent Robots and Systems (IROS)
October 25-29, 2020, Las Vegas, NV, USA (Virtual)

Improvement in measurement area of 3D LiDAR for a mobile robot using a mirror mounted on a manipulator

Kazuki Matsubara[1], Keiji Nagatani[2] and Yasuhisa Hirata[3]

***Abstract*— Light Detection and Ranging (LiDAR) is widely employed in mobile robots to acquire environmental information. However, it has a limited laser irradiation direction and cannot measure the backside of an object. In this study, a method that expands the LiDAR measurement range to various directions using a mirror installed on the manipulator mounted on mobile robots is developed. As mirrors can easily be mounted on robots, this method is expected to have a wide range of applications. This paper also proposes a method for determining the mirror position and attitude to expand the measurement area to obtain target data. In addition, we conducted an accuracy evaluation test of the reflection acquisition point. Using the proposed method, we demonstrate the measurement of the shape of descending staircase as an example of a potential application.**

Fig. 1. Mobile robot Quince equipped with a lightweight manipulator

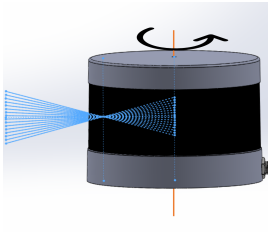

Fig. 2. LiDAR used in this study. By emitting multiple lasers in the vertical direction and rotating them around the central axis, omnidirectional point clouds can be obtained.

I. Introduction

Recently, demand for automation of plant inspection by employing robot technology has increased [1]. The necessity of reducing labor and ensuring safety is the reason for this increasing demand. In particular, companies with offshore platforms aim to employ mobile robots for autonomous inspection to avoid the burden on workers and the high cost of labor. Such robots need to generate environment map and estimate their own positions during autonomous driving. For these purposes, Light Detection and Ranging (LiDAR) is widely used. In particular, an omnidirectional 3D LiDAR instrument can acquire a 3D point cloud of the surrounding environment. This is significantly useful information that enables autonomous navigation of mobile robots.

In such mobile robots, a LiDAR instrument is typically installed at a position where the surrounding environment information can be acquired to the maximum possible extent, such as at the top of the robot body. Therefore, there are risks such as collision with obstacles and falling downstairs. To address this problem, moving the LiDAR instrument and mounting another sensor for short-range measurement have been proposed [2] [3]. However, these changes cannot be applied to robots that cannot incorporate additional moving parts or sensors. To solve this problem, we installed a mirror in an unused area of the LiDAR instrument, thereby expanding the measurement range in front of the robot, rather than installing additional moving parts and sensors [4]. However, only the measurement range for a region determined in advance can be extended using a fixed mirror. Therefore, it was not possible to measure undetermined areas.

However, a few mobile robots have a manipulator mounted on the upper part of the body to perform complicated tasks. Figure 1 shows the mobile robot Quince with a small manipulator developed by our research group. By using the manipulator, the position and orientation of the gripper mounted on the tip to grip objects that are close to the robot can be controlled. In addition, by installing tools such as grippers on the manipulator as well as observation equipment such as cameras and LiDAR, the measurement range of these observation instrument can be expanded [5] [6]. In this study, we focused on combining a manipulator, an observation equipment, and a mirror. Specifically, we propose a method for reflecting the laser emitted from the LiDAR instrument mounted on the robot, using a mirror installed on the manipulator. By installing a mirror at the base of the end effector, the measurement range can be expanded to various directions. This method involves lower installation costs and is less affected by the wiring and size of a LiDAR instrument compared to the method in which a LiDAR instrument is added to the manipulator. Therefore, it can be easily introduced into existing robots equipped with LiDAR instrument and manipulators in the main body.

In this study, a method for determining the position and orientation of the mirror with respect to the area to be measured was developed. In addition, an accuracy evaluation test to verify the effectiveness of the proposed determination method was conducted. Finally, this method was used to measure the shape of a descending staircase as an example application.

[1]The graduate school of engineering, Tohoku University, 6-6-10, Aramaki-Aoba, Aoba-ku, Sendai, 980-8579, Japan kazuki_matsubara@mhi.co.jp

[2]The University of Tokyo, 7-3-1 Hongo, Bunkyo-ku, Tokyo, 113-8656, Japan keiji@ieee.org

[3]Department of Robotics, Tohoku University, 6-6-10, Aramaki-Aoba, Aoba-ku, Sendai, 980-8579, Japan hirata@srd.mech.tohoku.ac.jp

II. Proposal of Mirror Position/Posture Determination Method

This method can extend the LiDAR measurement range to various directions. However, the position and orientation of the mirror reflecting the laser to the area to be extended are not always uniquely determined. In this section, we propose a cost function to determine the mirror position and orientation.

A. Cost function for determining mirror position and orientation

There are several cost functions for uniquely determining mirror position and orientation; however, they can be broadly classified into the following two types: cost functions based on manipulators and cost functions based on points acquired from a LiDAR. Manipulability, which was proposed by Yoshikawa, can be considered as a cost function based on the manipulator [7]. Manipulability is an index related to the operability of the manipulator. Moreover, it indicates the movability of the end-effector and is a type of distance from the singular configuration. When a series of poses is required for one task, such as grasping an object, a manipulator-based cost function should be used. However, in the proposed method, when measuring the 3D shape of an object, multiple mirror poses are assumed to be combined discontinuously. Therefore, in this study, we employed a cost function based on the points acquired from LiDAR.

For the cost function based on the acquired point cloud from LiDAR, parameters such as the size of the area where the acquired point cloud extends and the density of the acquired cloud point can be considered. Among them, we specially focus on the position accuracy of the acquired point cloud. In this study, we used a manipulator mounted on a mobile robot, as shown in Figure 1. As the manipulator is mounted on a mobile robot, it should be lighter than a normal manipulator. Thus, it has low rigidity and is prone to errors in the position and orientation of the end-effector. However, as shown in Figure 3, a plane-symmetric transformation using the mirror surface information needs to be applied to the position acquired by the laser reflected on the mirror. If the mirror information used in the calculation contains an error, the position obtained by the reflected laser cannot be converted to one that the reflected laser has actually reached. If the mirror is fixed, these errors can be eliminated through calibration in advance. However, with this method, it is difficult to perform calibration because the position and orientation of the mirror surface change depending on the target are to be expanded. Therefore, in this method, the position accuracy of the acquired point cloud is adopted as the cost function to determine mirror position and orientation.

B. Definition and calculation of the cost function

In this section, we define and calculate the cost function determined in the previous section. The cost function is the positional accuracy of the acquired point cloud, i.e., the position error of the acquired point cloud at a certain mirror surface. Let R be the arrival point of the laser reflected in the mirror and R' be the arrival point of the laser calculated on the mirror surface including the error. In this case, the position error of the acquisition point, which is a cost function, can be expressed as the magnitude of the vector connecting these two points. Assuming this vector to be $\Delta \boldsymbol{r}$, we define it as the cost function by the following equation.

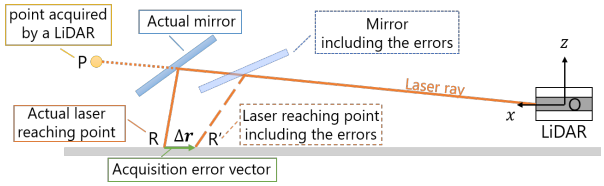

Fig. 3. Acquisition error vector generated when transforming the acquired points from LiDAR using the mirror information containing errors $\Delta \boldsymbol{r}$.

$$|\Delta \boldsymbol{r}| = |\overrightarrow{OR'} - \overrightarrow{OR}| \tag{1}$$

Next, we explain how to calculate the cost function. As explained in the previous section, a laser point reflected in a mirror surface can be obtained by using the mirror information and transforming it. As shown in Figure 3, we assume P to be the laser arrival point detected by LiDAR. In addition, let $\boldsymbol{n}$ be the normal vector of the mirror surface, and $\boldsymbol{q}$ be the position vector of the mirror surface. Furthermore, we assume $\boldsymbol{n}'$ and $\boldsymbol{q}'$ to be the position vector and the normal vector of the mirror surface including the error respectively. At this time, the vector $\overrightarrow{OR}$ from the point O of the laser to the point R of the laser reflected by the mirror can be expressed by Equation 2.

$$\overrightarrow{OR} = \overrightarrow{OP} + 2|\boldsymbol{n} \cdot (\overrightarrow{OP} - \boldsymbol{q})|\boldsymbol{n} \tag{2}$$

In the same way, the vector $\overrightarrow{OR'}$ from the laser ejection point O to the laser arrival point R', calculated with the mirror surface including the error, can be expressed by equation 3.

$$\overrightarrow{OR'} = \overrightarrow{OP} + 2|\boldsymbol{n}' \cdot (\overrightarrow{OP} - \boldsymbol{q}')|\boldsymbol{n}' \tag{3}$$

As the mirror is fixed on the manipulator, these errors can be calculated by the attitude estimation error of the manipulator. Several previous studies have determined the magnitude of the error that occurs in the end-effector for a certain manipulator posture [8] [9]. However, in the present study, we decided to use the method proposed by Wu [10]. Wu proposed a method for calculating the kinematic error of a link when the error was set for each of the DH link parameters. Using this method, it is possible to calculate an error occurring on a mirror surface in a certain manipulator posture. From the above, the acquisition point error $|\Delta \boldsymbol{r}|$, which is the cost function, can be calculated using Equations (1), (2), and (3), and the errors can be calculated by the method proposed by Wu.

III. Manipulator Attitude Calculation Method

Using the cost function defined in section II, the position and orientation of the mirror surface for the target can

be determined. In other words, the manipulator attitude can be uniquely determined. In the proposed method, the measurement targets are not only the measurement range and the angle of laser entry into the measurement range, but also tolerances. We can define the target position as the center position of the expanded measurement range and the target angle as the angle at which the laser enters the target position. Furthermore, we assume these tolerances be the position tolerance and angle tolerance, respectively. By allowing for tolerances in the measurement target, the optimal posture can be selected from among multiple manipulator postures that measure the target. On the other hand, the presence of many attitudes that measurement the target is problematic because it significantly increases the computation time of the cost function. In order to apply this method in various environments, it is desirable that the attitude of the manipulator with respect to the target is calculated in real time. To calculate it, examining the convexity of the cost function might be optimized. However, it is very difficult to examine the convexity of the cost function because the target position and target angle change. In this section, we propose a method to compute the solution in real time by limiting the positional posture of the cost function calculation for the measurement target, thereby reducing the computational time.

A. Determination of mirror position and orientation

The process of determining the mirror position and orientation with respect to the measurement target can be divided into the following three stages:

- setting measurement targets
- limiting the position and posture of the mirror surface to calculate the cost function
- computing the cost function

In the first stage, we set the target position and target angle, and their respective errors. In the second stage, the computational cost is lowered by reducing the number of computations of the cost function. In the third stage, we compute the cost function as defined in section II and uniquely determine the mirror position posture. In this section, we describe the second stage in detail. Note that the LiDAR used is assumed to be capable of emitting multiple lasers in the vertical direction and rotating them around an axis to acquire the surrounding 3D point cloud, as shown in Figure 2.

B. Limiting the position and orientation of the mirror surface to compute the cost function

In the second stage, we limit the position and posture of the mirror surface on which we compute the cost function. We defined this mirror surface that calculate the cost function as the mirror surface candidate. This stage allows a significant reduction in computational costs and allows the proposed method to be used in real time.

First, the laser that enters the target position at the target angles is termed as the target laser. We chose a laser that reflects at the center of the mirror surface from among many other reflective lasers because it is least likely to deviate from the mirror surface when the mirror position deviates from the target. A laser approaching the target position at a target angle is called a target approach laser.

When the targets are set, the mirror surface candidate satisfies the following two conditions, which are called the mirror candidate conditions:

- The minimum distance between the target laser and the target point is within the position tolerance (hereinafter referred to as the position condition)
- The angle between the target laser and target angles is within the angle tolerance (hereinafter referred to as the attitude condition)

The target lasers of all mirror surface candidates satisfy these conditions. Thus, the computational complexity can be reduced by computing the cost function only on the mirror surface candidates. When narrowing down the candidate mirror surfaces, we restrict the positions that become mirror surface candidates, and then select the postures that become the candidates at those positions. In this way, it is no longer necessary to calculate the mirror candidate conditions at all points of the calculation. In section III-B.1, we explain in detail how to limit the positions of mirror surface candidate, and in section III-B.2, we explain in detail how to select the orientation of mirror surface candidate.

1) Restricting positions that can be mirror surface candidates: First, we propose a method that limits the position where the mirror candidate condition is calculated. The position that can be the mirror candidate is hereinafter referred to as the calculation point. The calculation points satisfy the following two conditions:

- There is at least one mirror attitude that satisfies the mirror candidate conditions.
- The laser emitted from the LiDAR instrument reaches the mirror center.

First, a region where a position satisfying the first condition may exist is shown in Figure 4. The sphere in the figure represents the range from the target position T to the position tolerance e_p. To satisfy the first condition, the target laser must be in contact with this sphere at one point, at least, within the range satisfying the angle tolerance e_a Therefore, the position $\boldsymbol{x}$ that satisfies this condition exists inside the cone that inscribes the sphere and whose central axis is the target laser. When $\boldsymbol{l}_t$ is a unit vector representing the target approach angle, the first condition can be expressed as Equation 4.

$$\frac{\boldsymbol{c} \cdot (\boldsymbol{x} - \overrightarrow{OT} + \frac{e_p}{\sin e_a}\boldsymbol{l}_t)}{|\frac{e_p}{\tan e_a}|} \leq \cos e_a \tag{4}$$

The second condition is that a certain point $\boldsymbol{x}$ exists on the curved surface traced by the laser emitted from the LiDAR instrument (hereinafter referred to as the laser surface). As the LiDAR instrument emits the laser discretely, as shown in Figure 2, only the position that the laser can reach is treated as a calculation point. The existence of point $\boldsymbol{x}$ on the laser surface is equivalent to that of point $\boldsymbol{x}$, as the points are within tolerance d_l from the laser surface. Therefore,

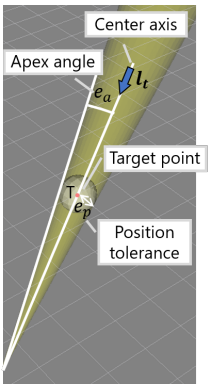

Fig. 4. Position where at least one mirror posture satisfying the mirror surface candidate condition exists in the cone.

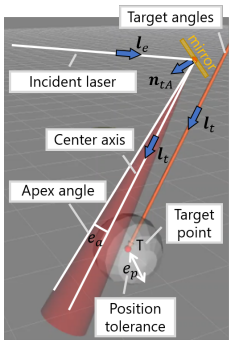

Fig. 5. Target laser that satisfies the attitude condition traces a cone with the calculation point at the vertex, vector representing the target angles at the center axis, and angle tolerance at the apex angle.

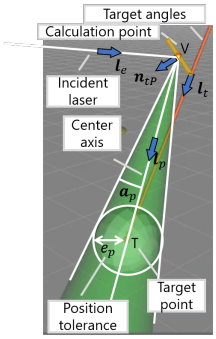

Fig. 6. Target laser traces a cone whose vertex is the calculation point. The cone inscribes a sphere whose center is the target point and radius is the position tolerance.

assuming $\boldsymbol{b}$ to be a unit vector from point $\boldsymbol{x}$ to the foot of the perpendicular traced down to the laser surface, the following equation holds:

$$d_l \geqq |\overrightarrow{OA} - (\boldsymbol{b} \cdot \overrightarrow{OA})\boldsymbol{b}| \tag{5}$$

The position that meets the second condition satisfies Equation (5) for at least one of the multiple laser surfaces.

From the above, the position that satisfies Equations 4 and 5 can be a mirror surface candidate.

2) Restricting orientations that can be mirror surface candidates: Next, we explain how to select a posture as a mirror surface candidate from among the calculation points. As in section III-B.1, we selected an orientation from among the calculation points using the mirror candidate condition.

The mirror normal vector $\boldsymbol{n}$ that realizes a certain reflected laser can be expressed as shown in Equation (6), where $\boldsymbol{l}_e$ is the incident laser vector, and $\boldsymbol{l}_r$ is the reflected laser vector.

$$\boldsymbol{n} = -\boldsymbol{l}_e + \sin\theta(\cos 2\theta \boldsymbol{l}_e + \boldsymbol{l}_r) \tag{6}$$

Here, θ is the angle of incidence and reflection on the mirror surface of the laser, which is represented by $2\theta = \cos^{-1}(-\boldsymbol{l}_e \cdot \boldsymbol{l}_r)$. Using Equation (6), the range of the mirror orientation that satisfies the angle and position conditions is determined.

First, we derive the range of the posture that satisfies the attitude condition. According to the attitude condition, the angle between the target laser and the vector representing the target angles is within the angle tolerance. In other words, the target laser that satisfies the attitude condition traces a cone with the calculation point at the vertex V, vector representing the target angles at the center axis, and angle tolerance at the apex angle, as shown in Figure 5. Assuming that $\boldsymbol{n}_{tA}$ is the mirror normal vector when the angle of the target laser is equivalent to the target angles, $\boldsymbol{n}_{tA}$ can be expressed as equation (7).

$$\boldsymbol{n}_{tA} = -\boldsymbol{l}_e + \sin\left\{\frac{\cos^{-1}(-\boldsymbol{l}_e \cdot \boldsymbol{l}_t)}{2}\right\}\{(-\boldsymbol{l}_e \cdot \boldsymbol{l}_t)\boldsymbol{l}_e + \boldsymbol{l}_t\} \tag{7}$$

Therefore, assuming $\boldsymbol{n}$ as the mirror normal vector and e_a as the angle tolerance between $\boldsymbol{n}$ and $\boldsymbol{n}_{tA}$, the range of $\boldsymbol{n}$ that satisfies Equation (8) becomes the range of posture that satisfies the attitude condition.

$$e_a \geqq \cos^{-1}\left(\frac{\boldsymbol{n}}{|\boldsymbol{n}|} \cdot \frac{\boldsymbol{n}_{tA}}{|\boldsymbol{n}_{tA}|}\right) \tag{8}$$

Next, we derive the range of the posture that satisfies the position condition. According to the position condition, the minimum distance between the target laser and the target point is within the position tolerance. Thus, the target laser traces a cone whose vertex is the calculation point, as shown in Figure 6. Note that the cone inscribes a sphere whose center is the target point and radius is the position tolerance. The central axis vector $\boldsymbol{l}_p$ and apical angle a_p of this cone can be described as in Equation (9), with the calculation point V as the vertex.

$$\boldsymbol{l}_p = \frac{\overrightarrow{VT}}{|\overrightarrow{VT}|} \quad a_p = \sin^{-1}\left(\frac{e_p}{|\overrightarrow{VT}|}\right) \tag{9}$$

Using Equations (6) and (9), similar to the attitude condition, the mirror normal vector $\boldsymbol{n}_{tP}$ satisfying the position condition can be expressed as

$$\boldsymbol{n}_{tP} = -\boldsymbol{l}_e + \sin\left\{\frac{\cos^{-1}(-\boldsymbol{l}_e \cdot \boldsymbol{l}_p)}{2}\right\}\{(-\boldsymbol{l}_e \cdot \boldsymbol{l}_p)\boldsymbol{l}_e + \boldsymbol{l}_p\} \tag{10}$$

Thus, when the mirror normal vector $\boldsymbol{n}$ satisfies the position condition, Equation (11), which indicates that the angle between $\boldsymbol{n}$ and $\boldsymbol{n}_{tP}$ is within the allowable error a_p, holds.

$$a_p \geqq \cos^{-1}\left(\frac{\boldsymbol{n}}{|\boldsymbol{n}|} \cdot \frac{\boldsymbol{n}_{tP}}{|\boldsymbol{n}_{tP}|}\right) \tag{11}$$

From the above, the orientation satisfying Equation (8) and (11) among the calculation points is a mirror surface candidate.

IV. Verification Test

A test was performed to verify the effectiveness of the proposed mirror position and orientation determination method.

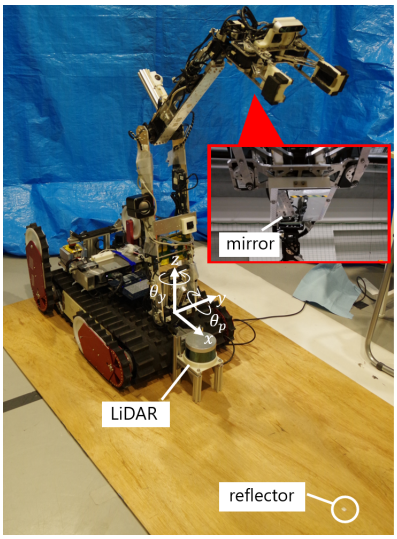

Fig. 7. Test environment. The reference coordinates were set so that the first joint axis of the manipulator coincides with the z-axis. The mirror was installed at the base of the end effector of the manipulator.

A. Test method

Figure 7 depicts the test environment. The mirror was installed at the base of the end effector of the manipulator, as shown in Figure 7. A lightweight manipulator Gestalt mounted on a mobile robot was used. Gestalt is a manipulator with six degrees of freedom and a maximum length of 1.45 m. In this test, only the errors of each joint angle were considered as the DH parameter error between each link of the manipulator, when calculating the acquisition point error. The error of each joint angle was defined as the backlash angle of the motor used in the experiment. VLP-16, which is manufactured by Velodyne Lidar, was used as the LiDAR instrument. Its primary specifications are listed in Table I.

The test procedure was as follows:

1) The targets and tolerances are set.
2) The following two postures are calculated for the target using the proposed method and are set as the target postures.
   - minimum posture: a posture that minimizes the cost function
   - maximum posture: a posture that maximizes the cost function
3) The manipulator is set to the base position shown in Figure 7.
4) The manipulator is set to the target posture and the reflection area is measured manually.
5) A reflector is placed as a landmark at a position where the reflected laser is expected to reach the ground.
6) Manually measure the position of the reflector.
7) Steps 3 and 4 are repeated three times for each target.

Based on the position of the reflector measured with the abovementioned procedure and the manually measured position, the acquisition error in each posture was calculated. Furthermore, the effectiveness of the proposed method was verified by comparing the acquired point errors calculated for the same target with the minimum and maximum postures.

TABLE I
SPECIFICATION OF VELODYNE VLP-16

Specification	Value
Number of lasers	16
Detection area	(Horizontal) 360°, (Vertical) ±15°
Measurement error	±3 cm (1 σ at 25 m)
Installation height	310 mm

TABLE II
TEST CONDITIONS

Conditions		Value
Position tolerance	(m)	0.02
Angle tolerance	(°)	5.0
Posture search point interval	(m)	0.025
Attitude search unit angle	(°)	1.0

B. Test conditions

Table II lists the tolerances and parameters for the manipulator posture search used in this experiment. Moreover, the target position and target angles relative to the reference coordinate system shown in Figure 7 were set under the following conditions.

- Fixed target angles: The target angles (θ_p, θ_y) were fixed at 0°, and the target position was set as follows:
  - $x = 600$ mm, 800 mm
  - $y = -300$ mm, 0 mm, 300 mm
  - $z = -136$ mm
- Fixed target position: The target position (x, y, z) was fixed to (800 mm, 0 mm, −136 mm), and the target angles were set as follows:
  - $\theta_p = 20°$
  - $\theta_y = 0°, \pm 45°, \pm 90°$

C. Results and discussion

Tables III and IV present the average values of the acquisition errors measured under each condition. In the tables, "minimum" represents the value for the minimum posture, and "maximum" represents the value for the maximum posture. The means and standard deviations (σ) of the acquisition errors for the two postures under all conditions are as follows:

- minimum posture
  - Average error: 30mm
  - σ: 13mm
- maximum posture
  - Average error: 50mm
  - σ: 25mm

These results indicate that the minimum attitude determined with the proposed method has a smaller acquisition error, regardless of the target position and target angle. However, the value obtained by multiplying σ with three and then adding the result to the average value is 70 mm for the case with minimum posture. This value is larger than that obtained

with the conventional LiDAR measurement. This is attributed to the errors in setting the LiDAR instrument and landmarks and the errors in the position and orientation of the end-effector due to low manipulator rigidity. Therefore, when acquiring mirror surface information, besides estimating the mirror surface posture from each joint angle of the manipulator, it may be necessary to estimate the mirror surface using multiple methods.

V. Potential Application of the Proposal Mechod

When a tracked vehicle inspects a plant, it will find traversing stairs particularly difficult. It is difficult to climb stairs because, in the case of a standard LiDAR placement, environmental information cannot be obtained for short-range distances. Therefore, when the tracked vehicle autonomously climbs down the stairs, the stair shape is acquired using other sensors or by measuring the stairs in advance. However, by employing the proposed method, the robot can measure the shape of the stairs in the downward direction, using the LiDAR instrument installed in the usual position. In this section, we demonstrate the measurement of the shape of a descending staircase as an example of a potential application of the proposed method.

A. Acquiring 3D shapes in a wide range

The number of lasers that can be reflected at once by this method is small, because the mirror is not very large and is far from the LiDAR instrument. Hence, when acquiring the 3D shape of the object, we used an approach in which measuring the point clouds reflected from multiple mirror positions and orientations were measured. In this test, multiple target positions and target angles were set near the descending stairs. Thereafter, for each measurement target, the mirror position and orientation were obtained using the proposed mirror position and orientation determination method. Finally, the point cloud around the measurement target point was acquired by moving the mirror surface around each mirror position and orientation.

B. Test method

Figure 8 illustrates the test environment. The manipulator and LiDAR instrument used in this experiment were the same as those mentioned in section IV. A total of nine measurement targets were set near the descending stairs, and we attempted to acquire the 3D shape of the stairs.

TABLE III

Average values of the acquisition errors for each target position for fixed target angles.

x (m)		0.6			0.8	
y (m)	-0.3	0.0	0.3	-0.3	0.0	0.3
minimum (m)	0.056	0.02	0.028	0.041	0.015	0.027
maximum (m)	0.067	0.023	0.031	0.104	0.025	0.033

TABLE IV

Average values of acquisition error for each target angle for fixed target positions.

θ_P (°)			20		
θ_y (°)	-90	-45	0	45	90
minimum (m)	34	29	19	10	42
maximum (m)	59	70	51	41	46

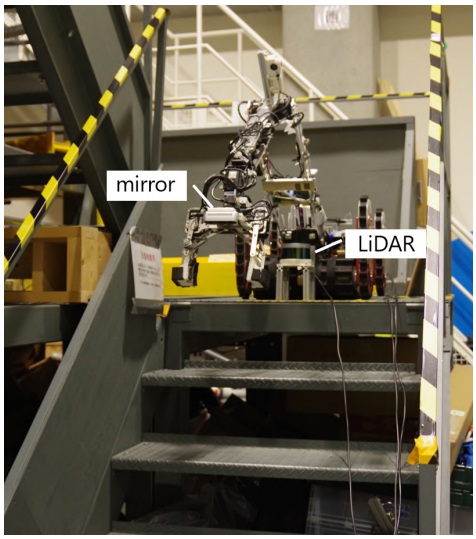

Fig. 8. Test environment for measuring the descending staircase. It is not possible to measure the shape of a descending staircase at the usual LiDAR instrument location.

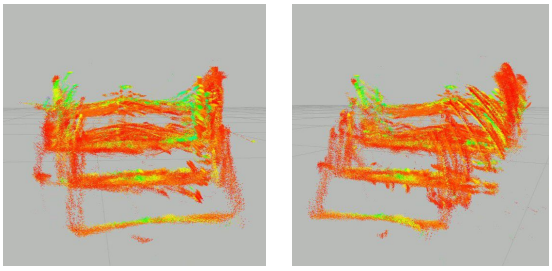

(a) View 1 (b) View 2

Fig. 9. Visualization of the points obtained using the mirror when measuring the shape of the descending stairs using the proposed method.

C. Measurement results and discussion

Figure 9 depicts the visualization result of the point cloud acquired using the mirror obtained in this test, after the removal of noise. For noise removal, we employed the StatisticalOutlierRemoval filter of the Point Cloud Library [11]. Views 1 and 2 were generated from the same data but different angles of view. Without the mirror system, almost all of the data in these figures vanishes, and it is impossible to obtain information about the stairs. The results indicate that the proposed method can measure the shape of the descending stairs, which cannot be measured using conventional methods. However, as the distance from the LiDAR instrument increases, the measured shape becomes distorted. In particular, the sidewall, which is expected to be a plane, is significantly distorted, as shown in Figure 9. This is attributed to the fact that the mirror surface information estimated from each joint angle of the manipulator and the actual mirror surface information are displaced. To obtain the stair information required for autonomous motion over

stairs, information that is more empirically accurate than the point cloud information obtained in this test is required. This indicates that it is necessary to consider more accurate mirror surface information acquisition method and implement measures such as distortion correction of the acquired point cloud.

VI. Conclusion

In this paper, we propose a method for expanding the measurement range of LiDAR by installing a mirror on a manipulator. We also propose a method and an index for determining the mirror position and orientation to expand the target measurement area. Moreover, a method for calculating the mirror position and orientation in real time is also described. Verification tests were conducted to confirm the effectiveness of the proposed cost function and the decision method. The results of the test revealed that the mirror conditions derived using the proposed decision method could be used to acquire a point cloud with a smaller acquisition error, as compared to other mirror conditions. Furthermore, as an example of an application in a real environment, a test was performed to acquire information about the shape of descending staircase. The results revealed that a point cloud representing a step could be acquired by merging the results obtained from multiple mirror positions and orientations. However, distortion occurred in the part where the acquisition error was large. Therefore, it is necessary to improve the mirror surface information acquisition method and to correct distortion of the acquired point cloud for practical applications. Future studies should focus on measuring a 3D shape with less distortion by acquiring mirror information with multiple methods and using a real environment.

ACKNOWLEDGMENT

This work was supported by Mitsubishi Heavy Industries, LTD. We would like to thank Editage (www.editage.com) for English language editing.

References

[1] L. Yu, E. Yang, P. Ren, C. Luo, G. Dobie, D. Gu, and X. Yan, "Inspection Robots in Oil and Gas Industry: a Review of Current Solutions and Future Trends," in *2019 25th International Conference on Automation and Computing (ICAC)*. IEEE, sep 2019, pp. 1–6. [Online]. Available: https://ieeexplore.ieee.org/document/8895089/

[2] Y. Okada, K. Nagatani, K. Yoshida, T. Yoshida, and E. Koyanagi, "Shared autonomy system for tracked vehicles to traverse rough terrain based on continuous T hree-dimensional terrain scanning," in *IEEE/RSJ 2010 International Conference on Intelligent Robots and Systems, IROS 2010 - Conference Proceedings*, 2010, pp. 357–362.

[3] K. Ohno, S. Tadokoro, K. Nagatani, E. Koyanagi, and T. Yoshida, "Trials of 3-D map construction using the tele-operated tracked vehicle kenaf at disaster city," in *2010 IEEE International Conference on Robotics and Automation*, 2010, pp. 2864–2870.

[4] K. Matsubara and K. Nagatani, "Improvement in measurement area of three-dimensional LiDAR using mirrors mounted on mobile robots," in *12th International Conference on Field and Service Robotics*, Tokyo, 2019, p. 13.

[5] P. Moubarak, P. Ben-Tzvi, Z. Ma, K. M. SUTHERLAND, and M. DUMAS, "A Mobile Robotic Platform for Autonomous Navigation and Dexterous Manipulation in Unstructured environments," in *Proceedings of the ASME International Mechanical Engineering Congress and Exposition (IMECE 2010)*, 2010.

[6] Qun Zhang, Shuzhi Sam Ge, and Pey Yuen Tao, "Autonomous stair climbing for mobile tracked robot," in *2011 IEEE International Symposium on Safety, Security, and Rescue Robotics*, 2011, pp. 92–98.

[7] T. Yoshikawa, "Manipulability of Robotic Mechanisms." *International Journal of Robotics Research*, vol. 4, no. 2, pp. 3–9, 1985.

[8] Jin-Oh Kim and K. Khosla, "Dexterity measures for design and control of manipulators," in *IEEE/RSJ International Workshop on Intelligent Robots and Systems '91*. IEEE, 1991, pp. 758–763.

[9] X. Zhou, Q. Zhang, W. A. Gruver, and G. Guo, "Distance and positioning accuracy for robotic manipulators," *IEEE/RSJ/GI International Conference on Intelligent Robots and Systems*, vol. 2, pp. 1399–1404, 1994.

[10] C. haur Wu, "Kinematic Error Model for the Design of Robot Manipulator." pp. 497–502, 1983.

[11] R. B. Rusu and S. Cousins, "3D is here: Point Cloud Library (PCL)," in *IEEE International Conference on Robotics and Automation (ICRA)*, Shanghai, China, 2011.